Journal of Power Sources 206 (2012) 91–96

Contents lists available at SciVerse ScienceDirect

Journal of Power Sources

journal homepage: www.elsevier.com/locate/jpowsour

The effect of an ultra-thin zirconia blocking layer on the performance of a 1-μm-thick gadolinia-doped ceria electrolyte solid-oxide fuel cell

Doo-Hwan Myung[a,b], Jongill Hong[b], Kyungjoong Yoon[a], Byung-Kook Kim[a], Hae-Weon Lee[a], Jong-Ho Lee[a], Ji-Won Son[a,*]

[a] High-Temperature Energy Materials Research Center, Korea Institute of Science and Technology, Hwarangno 14-gil 5, Seongbuk-gu, Seoul 130-791, Republic of Korea
[b] Dept. of Materials Science and Engineering, Yonsei University, 262 Seong Sanno, Seodaemun-gu, Seoul 120-749, Republic of Korea

ARTICLE INFO

Article history:
Received 19 December 2011
Received in revised form 16 January 2012
Accepted 19 January 2012
Available online 5 February 2012

Keywords:
Thin-film electrolyte solid-oxide fuel cell
Gadolinia-doped ceria
Pulsed laser deposition
Yttria-stabilized zirconia
Reduction-blocking layer

ABSTRACT

Ultra-thin (less than 200 nm) yttria-stabilized zirconia (YSZ) blocking layers are employed at the anode side of a 1-μm-thick gadolinia-doped ceria (GDC) thin-film electrolyte by pulsed laser deposition. Their effects on a GDC thin-film electrolyte solid-oxide fuel cell (TF-SOFC) are presented. Without blocking layers, the open cell voltage (OCV) of the GDC TF-SOFC is about 0.6 V. By inserting the blocking layer, the OCV increases to over 1 V. As a result, the maximum power density of the TF-SOFC increases from 377 mW cm^{-2} to over 1 W cm^{-2} at 600 °C. The present study demonstrates the possibility of obtaining the critical performance at a low temperature regime using thin-film GDC electrolytes.

1. Introduction

When minimizing the problems associated with high temperature operation, such as chemical reactions between the cell components and microstructural degradation, one of the key issues in the research of solid-oxide fuel cells (SOFCs) is the reduction of the operating temperature [1–4]. Low temperature operation is of significant technical importance to both conventional large-capacity and portable miniaturized SOFCs. It ensures reliability and cost-effectiveness, providing a pathway to commercialization of the former system [3,5], and facilitates thermal management, resulting in a reduction of size of the latter system [6,7]. In terms of the electrolyte, there are two key approaches to decrease the operating temperature: the first is to employ an alternative electrolyte material possessing higher ionic conductivity than that of the conventional electrolyte material, such as yttria-stabilized zirconia (YSZ) [1,3,5,8–13], and the second is to reduce the physical thickness of the conventional electrolyte to secure an appropriate conductance value of the electrolyte [6,14,15].

For an alternative material, doped ceria, such as gadolinia-doped ceria (GDC) and samaria-doped ceria (SDC), is the most studied material due to its high ionic conductivity at an intermediate temperature regime, chemical stability with Co-containing cathodes, and thermal expansion coefficient (TEC) match with adjacent Ni-cermet anodes [12,16]. Ceria-based electrolytes, however, become mixed conductors in the reducing condition because of the partial reduction of Ce^{4+} to Ce^{3+}, inducing cell voltage and efficiency loss due to internal short circuiting [9,11,16]. In addition, there can be further reduction of open circuit voltage (OCV) with a doped ceria electrolyte layer because the OCV of doped ceria is dependent on factors such as electrode materials and the thickness of the ceria layer as well; this is because the gradient of the defect concentration in the electrolyte is dependent on the operating condition [9,17]. It was proposed that, as both ionic and electronic fluxes increase with the decrease in thickness of the ceria electrolyte, OCV could drop further as a result of thin ceria electrolytes [9]. Therefore, employing a thick ceria electrolyte layer would be an obvious choice to suppress the additional OCV drop. Nonetheless, OCV deviation from theoretical predictions was observed even at thicknesses of approximately 30–40 μm [9,10,17]. This causes a dilemma in obtaining optimal performance of a SOFC with monolithic ceria electrolytes. To reduce ohmic loss, the thickness of the electrolyte should be reduced; however, the leakage current increases as the thickness decreases and, as a result, the SOFC output power inevitably decreases [9].

An actively studied approach to using a thin doped ceria-based electrolyte in SOFC reliably is to suppress electronic conduction of doped ceria by blocking its exposure to the reducing atmosphere [18]. A layer of a pure ionic conductor such as YSZ was coated at the

* Corresponding author. Tel.: +82 2 958 5530; fax: +82 2 958 5529.
E-mail address: jwson@kist.re.kr (J.-W. Son).

0378-7753/$ – see front matter © 2012 Elsevier B.V. All rights reserved.
doi:10.1016/j.jpowsour.2012.01.117

interface between ceria electrolytes and anodes to prevent ceria reduction; many reported an OCV increase near their theoretical values via the 'bi-layer electrolyte' approach [18–21]. Nevertheless, the performance reported for bi-layer electrolyte SOFCs was rather unsatisfactory; in some cases the power density was lower than that of the SOFC with a single layer ceria electrolyte [20]. When zirconia is used as the blocking layer, the thickness should be minimized because zirconia has an approximately 5 times higher resistance than that of ceria at 600 °C. For example, Zhang et al. [20] compared SOFCs with a 15-μm-thick SDC electrolyte and a 5-μm-thick YSZ + 15-μm-thick SDC bi-layer electrolyte. The YSZ layer had an equivalent resistance to a ceria layer approximately 25 μm thick so the bi-layer electrolyte had a factor of approximately 2.7 electrolyte resistance over the single layer ceria electrolyte in the reported case; thus, it is natural that the bi-layer electrolyte SOFC exhibited lower performance.

Therefore, to obtain improved performance using bi-layer electrolytes, it is necessary to fabricate a thin and continuous blocking layer between the ceria electrolyte and anode. It was predicted that only YSZ with a thickness of approximately 10^{-4} of that of GDC would be sufficient enough to protect GDC from reduction at 800 °C [18]. Though, it is extremely challenging to fabricate thin and dense layers using conventional powder processing; even if one uses thin-film processing, it is almost impossible to fabricate thin and continuous layers over porous and rough anode surfaces [6,22]. This could be the reason why there are few studies of successful applications of an ultra-thin blocking layer between the anode and the ceria electrolyte, especially in the anode-supported cells.

In previous studies [6,15], successful realizations of thin-film electrolyte SOFCs (TF-SOFCs) were possible due to surface modification of powder-processed anode supports. YSZ thin-film electrolytes, 1 μm in thickness, were well formed over anode supports through insertion of a nano-structure anode interlayer by means of a pulsed laser deposition (PLD). It is expected that this platform would enable the fabrication of an ultra-thin YSZ blocking layer with integrity for realizing high-performance thin-film GDC electrolyte anode-supported SOFCs, which is unprecedented. Therefore, this study observes the effects of fixing the thickness of the GDC electrolyte at 1 μm and at decreasing thickness of the YSZ blocking layer from 200 nm. The maximum thickness of YSZ was determined to be 200 nm because, at 600 °C, the resistance of 200-nm-thick YSZ is similar to that of 1-μm-thick GDC. This approach attempts to achieve both high OCV and power output of the GDC electrolyte cell.

2. Experimental

Tape-casted anode supports were used as the substrate for GDC-based TF-SOFCs. NiO and YSZ powders (NiO:8YSZ = 56:44 wt.%) and other additives were mixed to form the tape slurry. Tapes with thicknesses of approximately 300 μm were fabricated by tape casting. Three layers of tapes were laminated at 75 °C under a uniaxial pressure of 12.25 MPa. Sintering of the anode supports was performed at 1300 °C for 4 h in air. A detailed fabrication procedure is provided elsewhere [6].

On the 2 cm by 2 cm anode supports, a 4-μm-thick nano-structure NiO-YSZ interlayer, a YSZ blocking layer, a GDC electrolyte, and a 2-μm-thick lanthanum strontium cobaltite (LSC) cathode were sequentially fabricated using PLD. The YSZ and GDC layers covered the whole surface (2 cm by 2 cm) of the anode support. The dimension of the LSC cathode was 1 cm by 1 cm. The thickness of the GDC electrolyte was fixed as 1 μm and the thickness of the YSZ blocking layer was varied from 0 nm to 200 nm. Fabrication conditions for each thin-film component were identical to previous studies [6,15,22].

A custom-made button cell test set-up using a ceramic-glass composite-based compression seal was employed for unit cell tests [23]. For the cell test, air and 97% H_2/3% H_2O were used as the oxidant and the fuel, respectively, and the flow rates were kept at 200 sccm. The cell test temperature ranged from 350 °C to 600 °C, at intervals of 50 °C. Data measured at 600 °C are compared in the present study to exclude side effects from the sealing consistency [15]. Electrochemical properties such as IV characteristics and impedances of the TF-SOFCs were measured by means of a Solartron impedance analyzer with an electrochemical interface (SI1260 and SI1287, Solartron). The frequency range of the impedance analyses was 10^{-1}–10^{6} Hz. The microstructure of the cell was observed after the cell test using scanning electron microscopy (SEM, XL-30, FEI) and transmission electron microscopy (TEM, Technai G20, FEI).

3. Results and discussion

Fig. 1 shows the cross-sectional microstructures of the cells with different blocking layer thicknesses. Each figure on the left hand side shows a low-magnification figure of whole thin-film cell components; each figure on the right hand side shows a magnified image at the anode and electrolyte interface. Fig. 1(a) exhibits the microstructure of the cell without the blocking layer and clearly shows that the GDC electrolyte is directly exposed to the porous anode side. Figs. 1(b)–(e) are images of the cells with YSZ blocking layer thicknesses of 25, 50, 100, and 200 nm, respectively. In low-magnification figures, the cells appear similar to each other, with few differences in the microstructures and dimensions of the anode, GDC electrolyte, and cathode. In high-magnification figures, differences in the blocking layer thicknesses are more obvious. From the SEM figures, it can be concluded that the GDC-based TF-SOFCs were fabricated as intended, only to differentiate the blocking layer thicknesses.

For a closer observation, a TEM specimen was prepared in the 100 nm YSZ blocked cell using a focused ion beam (FIB); TEM observation was then performed. TEM images are displayed in Fig. 2. Fig. 2(a) shows a low magnification high angle annular dark field (HAADF) image of the overall structure; Fig. 2(b) shows a high magnification HAADF image at the anode–electrolyte interface. Fig. 2(c) is a bright field (BF) image at the anode–electrolyte interface. HAADF images (Fig. 2(a) and (b)) exhibit material contrast and show that a continuous YSZ layer was formed below the GDC layer. In the BF image (Fig. 2(c)), grain structures can be seen, showing the growth of a single grain of GDC on a single grain of YSZ, consistent with previous observations [24]. From TEM observations, it is noticeable that there are two epitaxial relations among the anode interlayer, the YSZ blocking layer, and the GDC electrolyte. The grain of YSZ blocking layer has a homoepitaxial relation with the YSZ grain of the anode interlayer. Therefore, the combined grain appears as one elongated grain (e.g. the grain at the center of Fig. 2(c), marked with a dashed line). On the other hand, the YSZ blocking layer on the pore generated by NiO to Ni reduction is not combined with NiO grains and shows the exact deposited thickness of the YSZ blocking layer (marked with a solid line). The YSZ grain at the blocking layer and the GDC grain at the electrolyte layer have a heteroepitaxial relation. The grains have the same crystallographic orientation with each other, but the interface appears clearly due to the difference in materials. These epitaxial relations further assist the microstructural integrity of the ultra-thin YSZ blocking layer.

These blocking layers significantly affected the OCV of the GDC-based cell. For each blocking layer thickness, three cells were fabricated and the OCV values of each cell at 600 °C are indicated in Fig. 3. There are three categories of the OCV values as a function of the blocking layer thickness. First, the OCV of the GDC

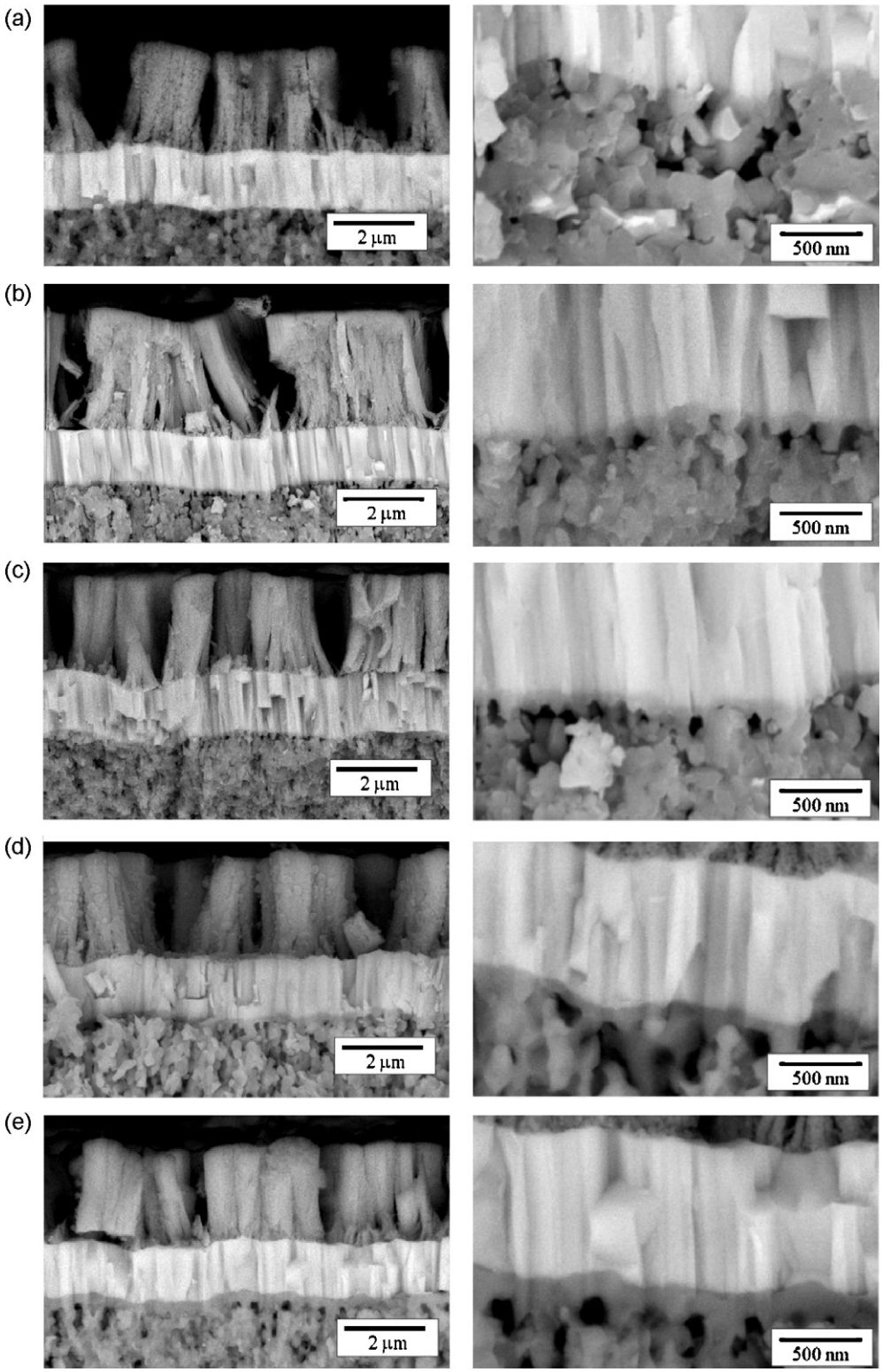

Fig. 1. Cross-sectional SEM micrographs of GDC-based TF-SOFCs. (a) Without a YSZ blocking layer, and with a (b) 25-nm, (c) 50-nm, (d) 100-nm and (e) 200-nm-thick YSZ blocking layer. Low-magnification figures are on the left hand side and high-magnification figures are on the right hand side.

TF-SOFC without the YSZ blocking layer exhibited OCV values lower than 0.6 V. This value is substantially lower than the calculated OCV of GDC (approximately 0.99 V) at 600 °C for the given fuel and oxidant compositions. In comparison with the experimentally obtained OCVs of cells with thicker monolithic ceria electrolytes [9,17,18], this OCV of the cell with a 1-μm-thick GDC electrolyte is significantly low as well. The result indicates that as the thickness of the GDC layer becomes as thin as 1 μm, additional phenomena induce further decreases of the oxygen partial pressure difference between the anode and cathode. As mentioned previously, this may be caused by oxygen permeation [9,17]. There is a possibility of physical leakage due to the thinness of the electrolyte. Based on

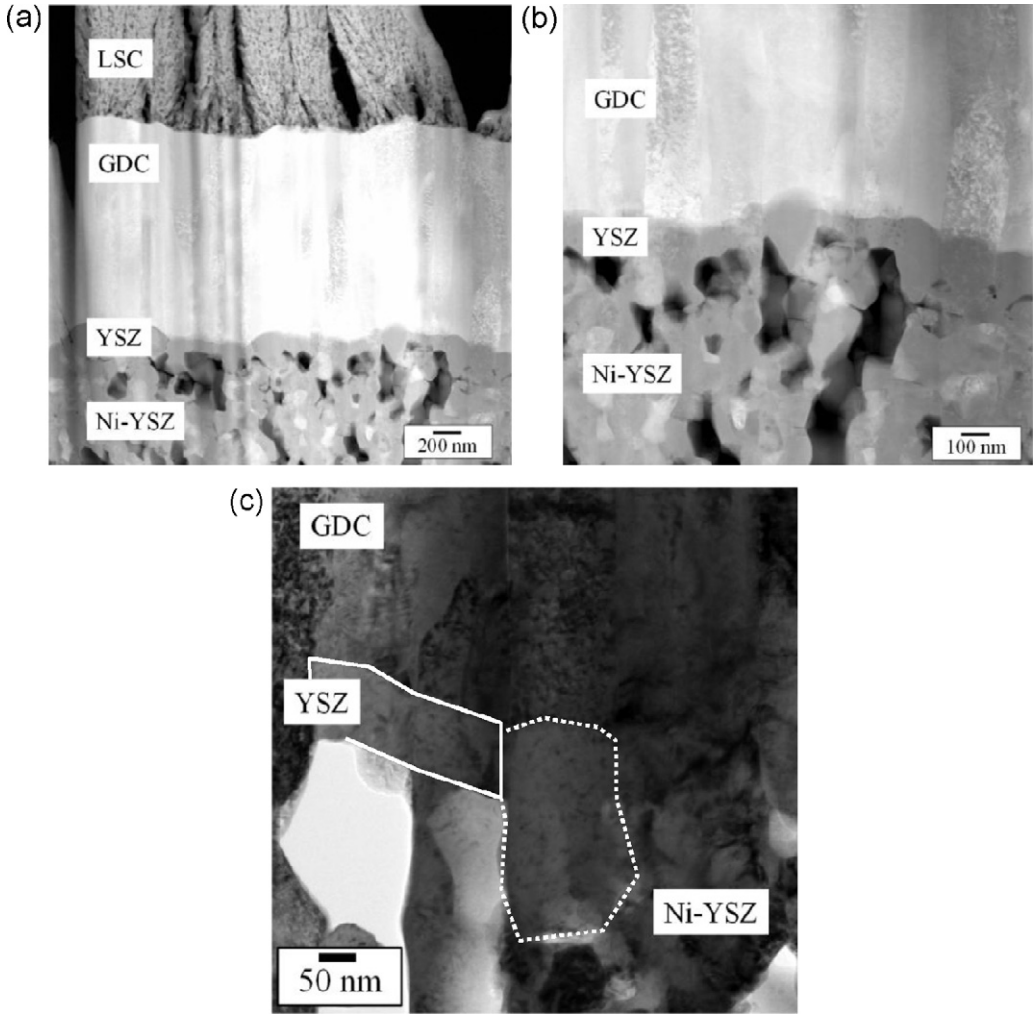

Fig. 2. (a) Low magnification and (b) high magnification HAADF images of 100-nm-thick YSZ blocked GDC TF-SOFC. (c) BF image at the anode–electrolyte interface.

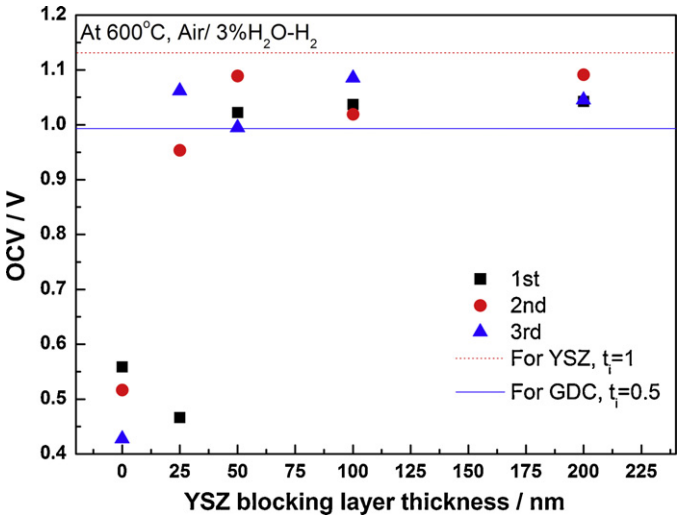

Fig. 3. Measured OCV values of the GDC-based cells at 600 °C as a function of the YSZ blocking layer thickness. The solid line indicates the calculated OCV of GDC at 600 °C when the transference number is 0.5 (i.e. the lower limit of the electrolytic domain of GDC). The dotted line indicates the calculated OCV of YSZ at 600 °C.

experience with thin YSZ electrolytes, however, 1-μm-thick electrolytes yield appreciable OCV values over the supported TF-SOFC design [6,15]. It is postulated that the structural integrity of the GDC electrolyte is comparable to that of the YSZ electrolyte; thus, the primary origin of further OCV deviation from its theoretical value is thought to be oxygen permeation through the GDC electrolyte.

Second, the insertion of the YSZ blocking layer substantially increased the OCV value of the cell from 0.6 V to over 1 V. Compared with other studies regarding the bi-layer electrolyte [18], the measured OCV values are in fair range, in spite of the extremely thin YSZ. This indicates that the ultra-thin YSZ blocking layers function appropriately; and this is the thinnest zirconia/ceria bi-layer combination ever reported that functions properly.

Third, the scattering of OCV values, however, is clearly noticeable for cells with thinner YSZ blocking layers. The degree of scattering diminishes as blocking layer thickness increases. As mentioned briefly, it was predicted that YSZ of 10^{-4} the size of the GDC thickness at 800 °C would prevent the reduction of GDC [18]. At 600 °C, the critical thickness reduces further. Following the methodology proposed by Kwon et al. [18], the thickness ratio of YSZ/GDC, t, can be calculated by:

$$t = \frac{t_{YSZ}}{t_{GDC}} = \frac{\sigma^*_{i,YSZ} \ln(P_{n,YSZ}^{-1/4} + (a^{II}_{O_2})^{-1/4})/(P_{n,YSZ}^{-1/4} + (a^{i}_{O_2})^{-1/4})}{\sigma^*_{i,GDC} \ln(P_{n,GDC}^{-1/4} + (a^{i}_{O_2})^{-1/4})/(P_{n,GDC}^{-1/4} + (a^{I}_{O_2})^{-1/4})} \quad (1)$$

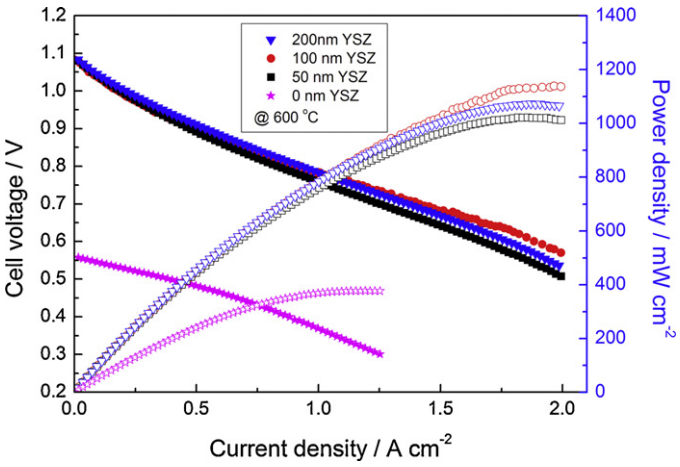

Fig. 4. *I–V–P* curves of GDC-based TF-SOFCs with various YSZ blocking layer thicknesses at 600 °C.

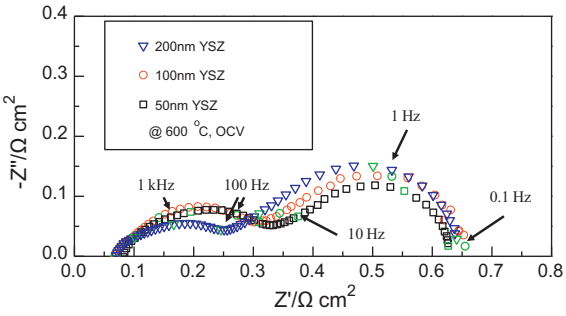

Fig. 5. Impedance spectra (IS) of GDC-based TF-SOFCs with various YSZ blocking layer thicknesses at 600 °C.

where σ_i^* denotes ionic conductivity of each material; P_n denotes the reducing bound in oxygen activity of each material; $a_{O_2}^{II}$ is oxygen activity at the fuel side, approximately 1.58×10^{-27} at 600 °C; $a_{O_2}^{I}$ is oxygen activity at the air side, approximately 0.21; and $a_{O_2}^{i}$ is oxygen activity at the GDC/YSZ interface. When $a_{O_2}^{i}$ is equal to or higher than $P_{n,GDC}$, the reduction of GDC is prevented. At 600 °C, $\sigma_{i,YSZ}^* = 4.5 \times 10^{-3}$ S cm^{-1}; $\sigma_{i,GDC}^* = 1.6 \times 10^{-2}$ S cm^{-1}; $P_{n,YSZ} = 1.94 \times 10^{-52}$; and $P_{n,GDC} = a_{O_2}^{i} = 2.04 \times 10^{-24}$ [25,26]. From these data, it is calculated that if the thickness ratio of YSZ/GDC is higher than approximately 2×10^{-7}, then the YSZ layer can block the GDC layer. This means that for 1-μm-thick GDC, an infinitesimally thin YSZ layer (thickness of approximately 2×10^{-3} Å) would be sufficient. All experimented YSZ thicknesses are much thicker than this value; thus, the observed scattering OCV values are not caused by failing to meet the aforementioned theoretical requirement.

This result indicates that successful realization of an ultra-thin, continuous, and gas-impermeable layer is hampered by fabrication conditions, not by theoretical limitations. Non-ideal OCV values of bi-layer electrolytes from numerous literatures [18], in spite of the sufficient thickness of the blocking layer, support that the processing limitations often govern the experimental results. In this study, the primary factor affecting the effective thickness of the blocking layer is believed to be the surface roughness of the deposition surface. The surface roughness of the deposition surface is determined by that of the anode support and the root-mean-square roughness (R_{rms}) of the tape-casted anode support, approximately 77 nm when measured by atomic force microscopy (AFM). As a kind of physical vapor deposition (PVD), PLD has a weakness in conformal step coverage. Therefore, the probability of non-uniform and incomplete coverage of the anode surface becomes higher when YSZ film becomes thinner than the dimension of the features at the deposition surface. This appears to be the reason for the scattering OCV values at thinner YSZ thicknesses. Additionally, anode supports with about twice the roughness of the tape-casted anode were used to confirm the effect of the surface roughness on the effective blocking layer thickness. The R_{rms} of the rougher anode support was approximately 144 nm. With the rougher anode support, even GDC TF-SOFCs with a 200-nm-thick YSZ blocking layer showed more scattered OCV values, with the lowest value reaching 0.9 V. This result demonstrated that the measured electrochemical properties of TF-SOFCs are determined by the fabrication condition such as the substrate surface roughness and process sequence.

The power output of each cell at 600 °C is compared in Fig. 4. The insertion of the blocking layer is remarkably effective in increasing the OCV and thus, the power output of the cell. The peak power density of the cell without the YSZ blocking layer was 377 mW cm^{-2} and those of cells with the YSZ blocking layer were higher than 1 W cm^{-2}. The substantial difference implies that the bi-layer approach should be considered as inevitable in employing thin-film GDC electrolytes.

Nevertheless, it was difficult to discern the dependency of the power output on the blocking layer thickness. By breaking down and comparing the ASR values, the reason for the little difference among the cells with various blocking layer thicknesses could be deduced. In Fig. 5, the impedance spectrum (IS) of each cell is shown. Noticeably, the ohmic ASR is much bigger than the electrolyte resistance. The ASRs of the 200 nm YSZ + 1 μm GDC, 100 nm YSZ + 1 μm GDC, and 50 nm YSZ + 1 μm GDC at 600 °C are approximately 0.0119, 0.0086, and 0.0075 Ωcm^2, respectively. These values were calculated using the conductivities of PLD YSZ and GDC thin films measured by a four-point probe measurement [27]. The ohmic ASRs are around 0.06 Ωcm^2, more than 5 times the contribution of electrolyte resistance, indicating there are significant ohmic resistance contributions from sources other than the electrolyte that increase ohmic loss. More importantly, the differences of electrolyte ASR among the cells are less than 10% of the total ohmic loss. Therefore, it is highly possible that other contributions to total ohmic loss would override the electrolyte ohmic loss; thus, it is more difficult to precisely reflect the effect of the electrolyte ohmic resistance variation on the cell performance.

In terms of the polarization ASR, it is noted that all of the cells compared in Fig. 5 exhibited similar overall polarization ASR values, because their electrode materials and structures were intended to be nearly identical. The polarization ASR values were estimated to be approximately 10 times that of the ohmic ASR. This means that polarization loss due to electrode activity dominates overall cell performance. This implies that the employment of ideal electrodes with extremely high electrochemical activity is necessary to assess the effects of delicate changes in the electrolyte configuration.

Nevertheless, the current study proves the effectiveness of the bi-layer electrolyte approach at an unprecedented thickness range. It is expected that critical low-temperature performances of SOFCs can be obtained with this state-of-the-art technology, provided that the losses from sources other than the electrolyte are able to be eliminated.

4. Conclusions

Ultra-thin YSZ blocking layers less than 200 nm in thickness are inserted in between a 1-μm-thick GDC electrolyte and anode support. By employing surface modification with a PLD nano-structure anode interlayer, the GDC-based TF-SOFC with ultra-thin and

continuous YSZ layers is successfully constructed. Insertion of the YSZ layer substantially increases the OCV. The YSZ blocking layer thickness that yields stable OCV values is dependent on the surface roughness of the anode substrate, suggesting that a successful realization of the working cell structure is substantially affected by the fabrication variables. By inserting the blocking layer, the cell performance significantly increases; thus, the bi-layer approach should be considered as essential in employing thin-film GDC electrolytes. Although other ohmic and polarization losses should be reduced to exactly assess the effect of the electrolyte resistance variation, the current study demonstrates the possibility of obtaining critical performance at a low temperature regime using thin-film GDC electrolyte with ultra-thin YSZ blocking layers.

Acknowledgements

This work was supported by the Institutional Research Project of the Korea Institute of Science and Technology (KIST) and the Global Frontier R&D Program on Center for Multiscale Energy System funded by the National Research Foundation under the Ministry of Education, Science and Technology, Korea (2011-0031579).

References

[1] S. Zha, C. Xia, G. Meng, J. Power Sources 115 (2003) 44–48.
[2] T. Suzuki, M.H. Zahir, T. Yamaguchi, Y. Fujishiro, M. Awano, N. Sammes, J. Power Sources 195 (2010) 7825–7828.
[3] D.H. Prasad, J.-W. Son, B.-K. Kim, H.-W. Lee, J.-H. Lee, J. Eur. Ceram. Soc. 28 (2008) 3107–3112.
[4] H.-Y. Jung, K.-S. Hong, H.-G. Jung, H. Kim, H.-R. Kim, J.-W. Son, J. Kim, H.-W. Lee, J.-H. Lee, J. Electrochem. Soc. 154 (2007) B480–B485.
[5] J.-H. Lee, K.-N. Kim, J.-W. Son, J. Kim, B.-K. Kim, H.-W. Lee, J. Moon, J. Mater. Sci. 42 (2007) 1866–1871.
[6] H.-S. Noh, H. Lee, B.-K. Kim, H.-W. Lee, J.-H. Lee, J.-W. Son, J. Power Sources 196 (2011) 7169–7174.
[7] C.-W. Kwon, J.-W. Son, J.-H. Lee, H.-M. Kim, H.-W. Lee, K.-B. Kim, Adv. Funct. Mater. 21 (2011) 1154–1159.
[8] T. Ishihara, H. Eto, J. Yan, Int. J. Hydrogen Energy 36 (2011) 1862–1867.
[9] K.L. Duncan, K.-T. Lee, E.D. Wachsman, J. Power Sources 196 (2011) 2445–2451.
[10] C. Ding, H. Lin, K. Sato, K. Amezawa, T. Kawada, J. Mizusaki, T. Hashida, J. Power Sources 195 (2010) 5487–5492.
[11] Y. Lee, J.H. Joo, G.M. Choi, Solid State Ionics 181 (2010) 1702–1706.
[12] L. Zhang, F. Chen, C. Xia, Int. J. Hydrogen Energy 35 (2010) 13262–13270.
[13] C. Ding, H. Lin, K. Sato, T. Hashida, J. Membr. Sci. 350 (2010) 1–4.
[14] B.C.H. Steele, A. Heinzel, Nature 414 (2001) 345–352.
[15] H.-S. Noh, J.-W. Son, H. Lee, H.-S. Song, H.-W. Lee, J.-H. Lee, J. Electrochem. Soc. 156 (2009) B1484–B1490.
[16] X. Zhang, M. Robertson, C. Deces-Petit, W. Qu, O. Kesler, R. Maric, D. Ghosh, J. Power Sources 164 (2007) 668–677.
[17] K.L. Duncan, E.D. Wachsman, J. Electrochem. Soc. 156 (2009) B1030–B1038.
[18] T.-H. Kwon, T. Lee, H.-I. Yoo, Solid State Ionics 195 (2011) 25–35.
[19] T. Tsai, E. Perry, S. Barnett, J. Electrochem. Soc. 144 (1997) L130–L132.
[20] X. Zhang, M. Robertson, C. Decès-Petit, Y. Xie, R. Hui, S. Yick, E. Styles, J. Roller, O. Kesler, R. Maric, D. Ghosh, J. Power Sources 161 (2006) 301–307.
[21] Q.L. Liu, K.A. Khor, S.H. Chan, X.J. Chen, J. Power Sources 162 (2006) 1036–1042.
[22] J.C. Kim, D.Y. Lee, H.-R. Kim, H.-W. Lee, J.-H. Lee, J.-W. Son, Thin Solid Films 519 (2011) 2534–2539.
[23] H.-S. Noh, J.-W. Son, H. Lee, J.-S. Park, H.-W. Lee, J.-H. Lee, Fuel Cells 10 (2010) 1057–1065.
[24] H.-S. Noh, J.-S. Park, H. Lee, H.-W. Lee, J.-H. Lee, J.-W. Son, Elecrochem. Solid State Lett. 14 (2011) B26–B29.
[25] S.-H. Park, H.-I. Yoo, Solid State Ionics 176 (2005) 1485–1490.
[26] J.-H. Park, R.N. Blumenthal, J. Electrochem. Soc. 136 (1989) 2867–2876.
[27] H.-R. Kim, J.-C. Kim, K.-R. Lee, H.-I. Ji, H.-W. Lee, J.-H. Lee, J.-W. Son, Phys. Chem. Chem. Phys. 13 (2011) 6133–6137.